Electronic Supplementary Information

Mechanism studies of addition reactions between the pyrimidine type radicals and their 3'/5' neighboring deoxyguanosines

Shoushan Wang[a, b], Min Zhang[b], Peng Liu[b], Shilei Xie[b], Faliang Cheng[b,*], Lishi Wang[a,*]

[a] School of Chemistry and Chemical Engineering, South China University of Technology, Guangzhou 510641, People's Republic of China.

[b] Guangdong Engineering and Technology Research Center for Advanced Nanomaterials, School of Environment and Civil Engineering, Dongguan University of Technology, Dongguan 523808, People's Republic of China.

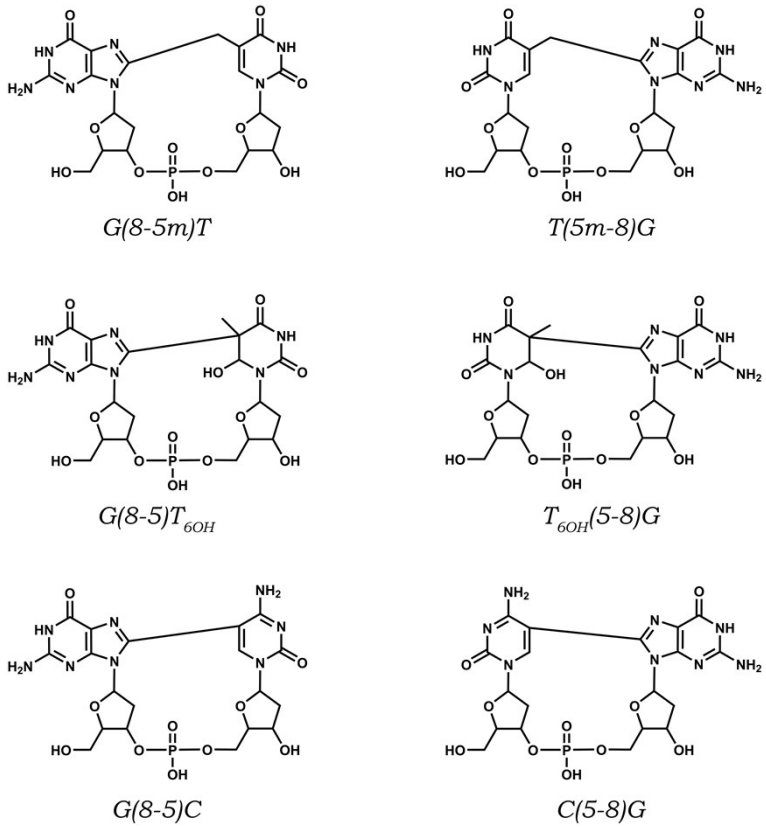

Figure S1 Prototype structures of the six related closed-shell DNA intrastrand cross-links.

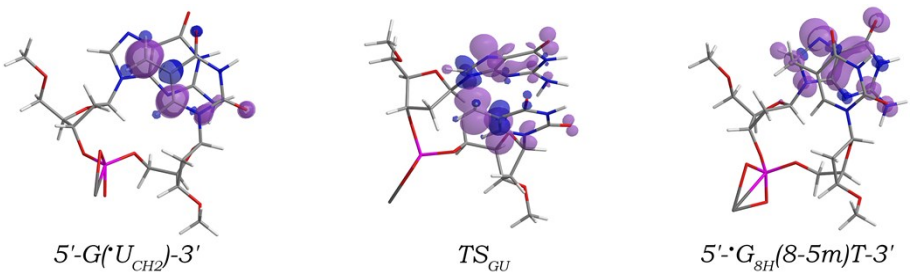

Figure S2 Spin density distributions of stationary points along the reaction path of the •U_{CH2} radical addition to the C_8 site of its 5' neighboring deoxyguanosine.

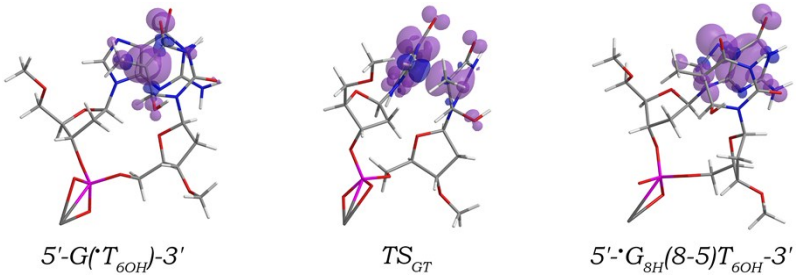

Figure S3 Spin density distributions of stationary points along the reaction path of the •T_{6OH} radical addition to the C_8 site of its 5' neighboring deoxyguanosine.

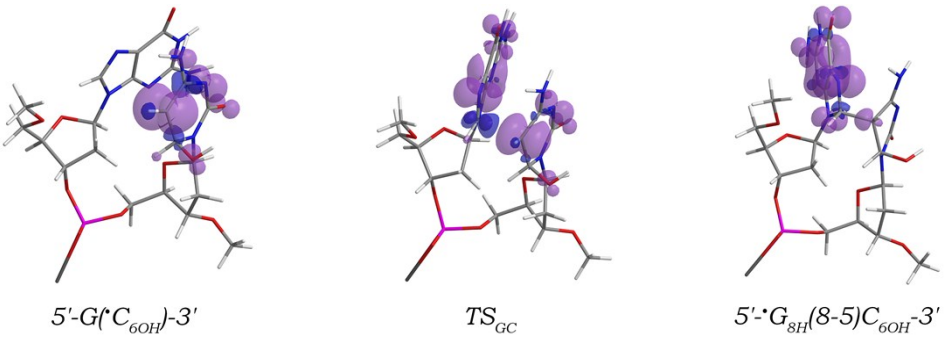

Figure S4 Spin density distributions of stationary points along the reaction path of the •C_{6OH} radical addition to the C_8 site of its 5' neighboring deoxyguanosine.

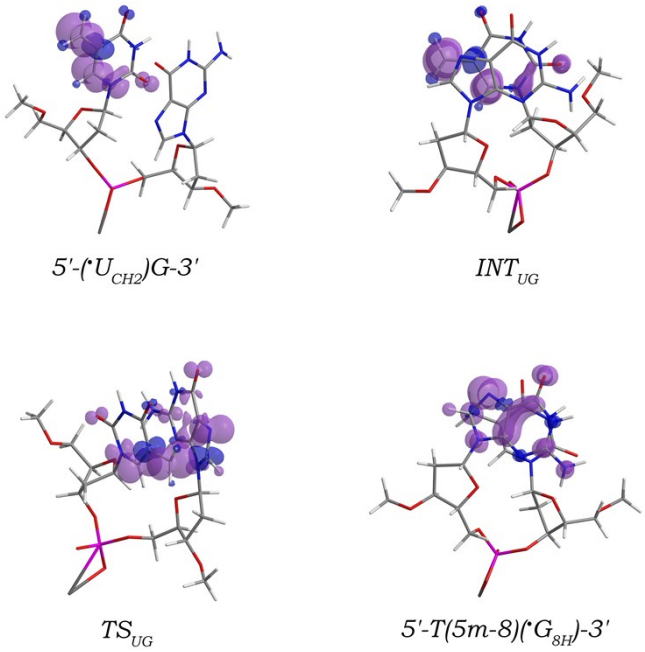

Figure S5 Spin density distributions of stationary points along the reaction path of the $^{\bullet}U_{CH2}$ radical addition to the C_8 site of its 3' neighboring deoxyguanosine.

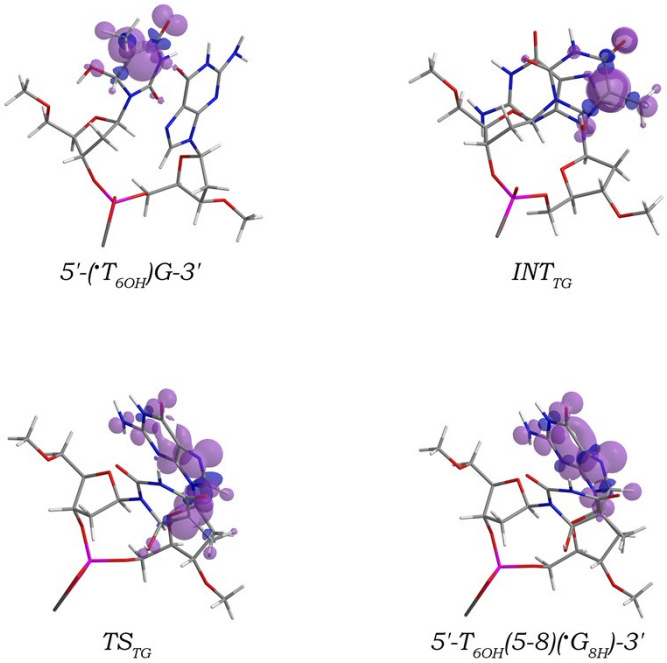

Figure S6 Spin density distributions of stationary points along the reaction path of the $^{\bullet}T_{6OH}$ radical addition to the C_8 site of its 3' neighboring deoxyguanosine.

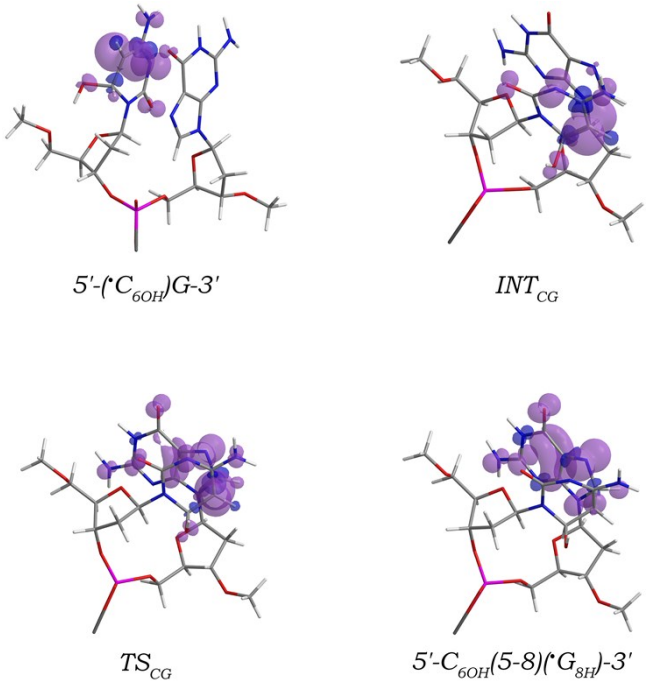

Figure S7 Spin density distributions of stationary points along the reaction path of the $^{\bullet}C_{6OH}$ radical addition to the C_8 site of its 3' neighboring deoxyguanosine.

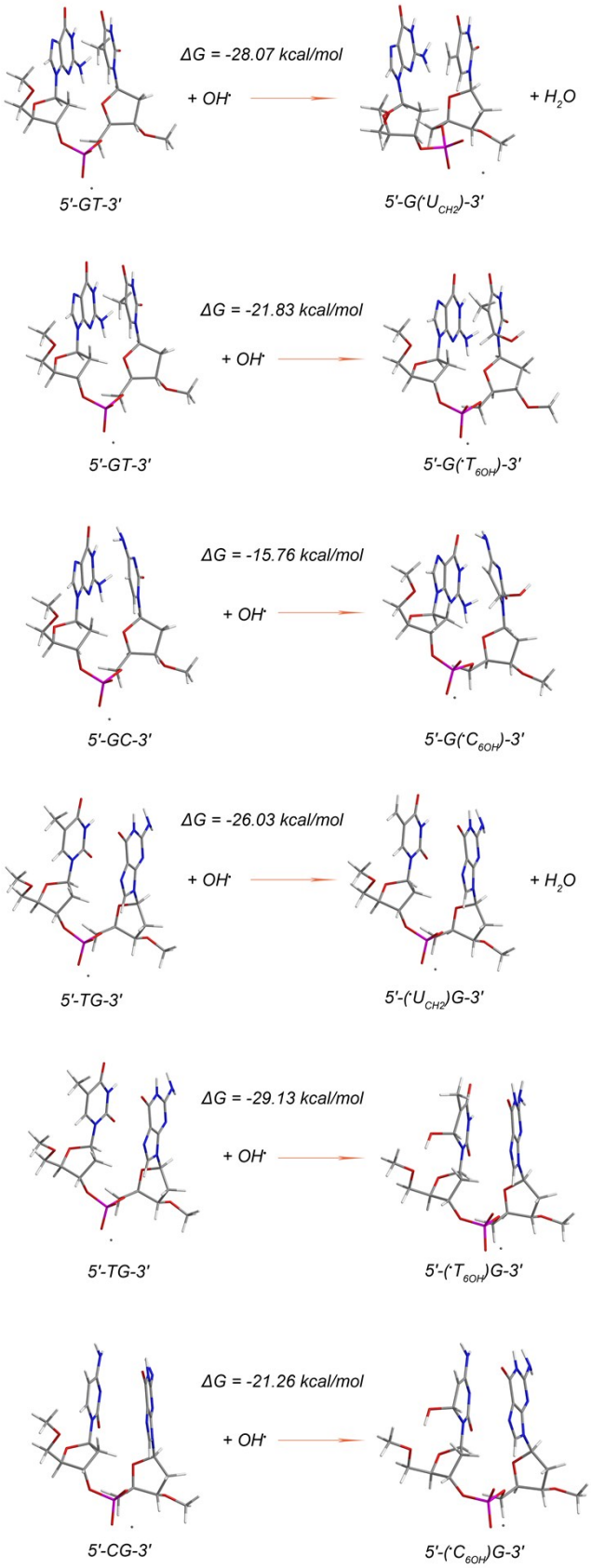

Figure S8 Reaction free energies calculated for the OH• radical reacting with the canonical 5'-GT-3', 5'-GC-3', 5'-TG-3', and 5'-CG-3' sequences forming the 5'-G(•U_{CH2})-3', 5'-G(•T_{6OH})-3', 5'-G(•C_{6OH})-3', 5'-(•U_{CH2})G-3', 5'-(•T_{6OH})G-3', and 5'-(•C_{6OH})G-3' sequences, respectively.

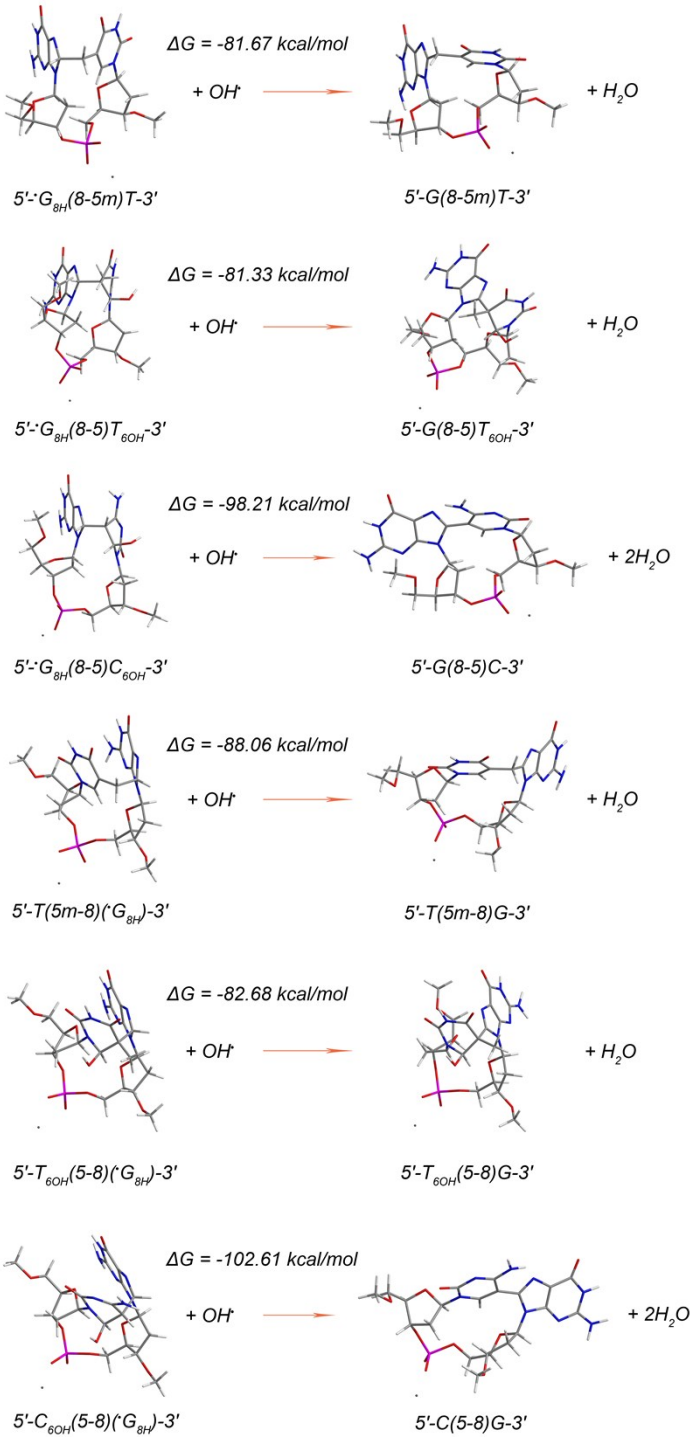

Figure S9 Reaction free energies calculated for formation of the closed-shell 5'-G(8-5m)T-3', 5'-G(8-5)T_{6OH}-3', 5'-G(8-5)C-3', 5'-T(5m-8)G-3', 5'-T_{6OH}(5-8)G-3', and 5'-C(5-8)G-3' intrastrand cross-links starting from the radical adducts, 5'-•G_{8H}(8-5m)T-3', 5'-•G_{8H}(8-5)T_{6OH}-3', 5'-•G_{8H}(8-5)C_{6OH}-3', 5'-T(5m-8)(•G_{8H})-3', 5'-T_{6OH}(5-8)(•G_{8H})-3', and 5'-C_{6OH}(5-8)(•G_{8H})-3', respectively.